Biosensors

Deutsche Ausgabe: DOI: 10.1002/ange.201508990
Internationale Ausgabe: DOI: 10.1002/anie.201508990

Programming A Molecular Relay for Ultrasensitive Biodetection through ^{129}Xe NMR

*Yanfei Wang, Benjamin W. Roose, John P. Philbin, Jordan L. Doman, and Ivan J. Dmochowski**

Abstract: *A supramolecular strategy for detecting specific proteins in complex media by using hyperpolarized ^{129}Xe NMR is reported. A cucurbit[6]uril (CB[6])-based molecular relay was programmed for three sequential equilibrium conditions by designing a two-faced guest (TFG) that initially binds CB[6] and blocks the CB[6]–Xe interaction. The protein analyte recruits the TFG and frees CB[6] for Xe binding. TFGs containing CB[6]- and carbonic anhydrase II (CAII)-binding domains were synthesized in one or two steps. X-ray crystallography confirmed TFG binding to Zn^{2+} in the deep CAII active-site cleft, which precludes simultaneous CB[6] binding. The molecular relay was reprogrammed to detect avidin by using a different TFG. Finally, Xe binding by CB[6] was detected in buffer and in E. coli cultures expressing CAII through ultrasensitive ^{129}Xe NMR spectroscopy.*

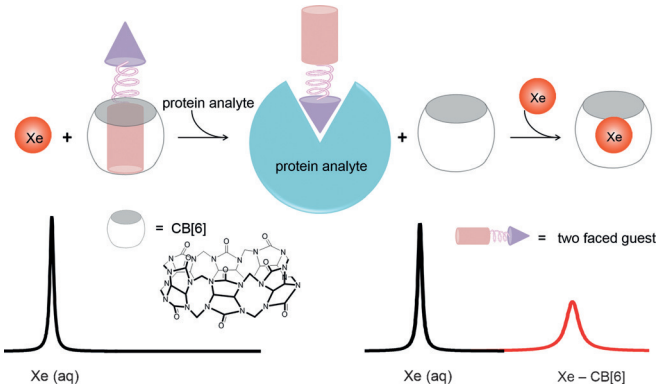

Scheme 1. Molecular relay produces an ^{129}Xe NMR signal upon analyte detection.

Methods for controlling the sequential interaction of molecules in solution can yield new functionality and complexity, as evidenced by many enzyme- and small-molecule-mediated tandem reactions, drug delivery strategies, and nanoscale and mesoscale architectures and working "machines".[1] Less investigated are supramolecular strategies for improving in situ sample analysis, e.g., for generating high contrast in bioassays and molecular imaging. Our group and Schröder's recently showed that commercially available cucurbit[6]uril (CB[6], Scheme 1) provides exceptional contrast at pM concentrations through hyperpolarized (hp) ^{129}Xe chemical exchange saturation transfer (Hyper-CEST) NMR.[2] In Hyper-CEST, encapsulated hp ^{129}Xe is selectively depolarized by radiofrequency pulses, and through rapid exchange, the depolarized ^{129}Xe accumulates in the solvent pool where the decrease in signal can be readily monitored (Scheme S1 in the Supporting Information).[3] CB[6] is not readily functionalized for biosensing applications, however. We thus exploited the versatile host–guest chemistry of CB[6] to develop a de novo "molecular relay" that reports on specific proteins in solution.

^{129}Xe NMR/MRI has enabled the investigation of many complex porous systems, from inorganic and organic materials[4] to bacterial spores[5] and mammalian lungs.[6] For the detection of specific proteins in solution, however, a specific encapsulating agent is required since Xe has low affinity for endogenous biomolecules. Cryptophane-A and its derivatives are the most studied Xe-binding cages and they exhibit the largest association constants.[7] However, cryptophane biosensors require multistep synthesis that yields only milligram quantities.[8] This has motivated the search for new ^{129}Xe-binding scaffolds.[9]

The rigid structure and unique molecular recognition properties of cucurbit[*n*]uril (CB[*n*]) compounds make these useful as drug delivery vehicles, chemical reaction chambers, components of enzyme assays, and building blocks in stimuli-responsive supramolecular architectures.[10,11] Importantly, CB[6] has a suitable cavity size to bind Xe ($D \approx 4.4$ Å), and CB[6] and a water-soluble derivative were reported to bind Xe with useful affinities ($K_A = 500$–$3000\ M^{-1}$ at RT).[12,2a] Herein, we describe CB[6]–^{129}Xe NMR biosensors programmed for a molecular relay with three sequential recognition events (Scheme 1). A two-faced guest (TFG) is engineered to control this relay, such that the CB[6]–^{129}Xe NMR signal is absent until addition of analyte.

CB[6] guest-binding affinities first measured by Mock and co-workers[13] guided our design of TFGs that bind CB[6] with intermediate affinity (displacing Xe) and are readily sequestered upon binding of the opposite TFG face to a higher-affinity protein target. Butylamine was measured by ITC to exhibit intermediate affinity for CB[6] ($K_A = 2.85 \times 10^5\ M^{-1}$ in pH 7.2, PBS solution at 300 K; Figure S1a in the Supporting Information). We chose human carbonic anhydrase II (CAII, EC 4.2.1.1) as the initial target because this is a model single-site enzyme with biomedical significance[14] and its inhibitors have been well studied.[15] The active site of CAII resides at the base of an approximately 15 Å deep conical pocket that can differentiate between TFGs even if they share the same

[*] Y. Wang, B. W. Roose, J. P. Philbin, J. L. Doman, Prof. I. J. Dmochowski
Department of Chemistry, University of Pennsylvania
231 South 34th Street, Philadelphia, PA 19104-6323 (USA)
E-mail: ivandmo@sas.upenn.edu

Supporting information and ORCID(s) from the author(s) for this article are available on the WWW under http://dx.doi.org/10.1002/anie.201508990.

Table 1: The two-faced guests (TFGs) used in this study and thermodynamic data for binding to CB[6], CAII, or avidin.

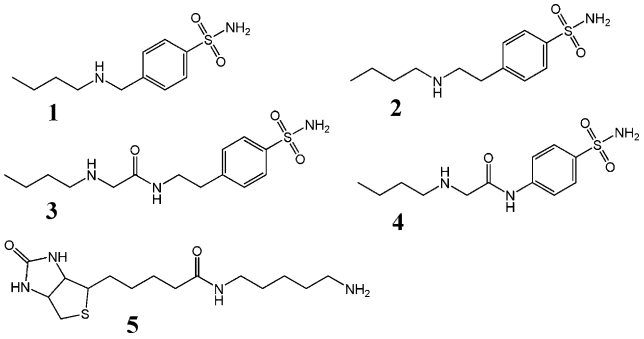

TFG	Host	K_D [μM]	ΔH [kcal mol^{-1}]	$T\Delta S$ [kcal mol^{-1}]	ΔG [kcal mol^{-1}]
1	CB[6]	4.07 ± 0.55	−1.17 ± 0.02	6.24	−7.41
	CAII	1.11 ± 0.29	1.23 ± 0.03	9.39	−8.16
2	CB[6]	6.58 ± 0.89	−0.91 ± 0.03	6.21	−7.12
	CAII	2.29 ± 0.46	−2.19 ± 0.08	5.55	−7.74
3	CB[6]	5.55 ± 0.72	−2.33 ± 0.05	4.89	−7.22
	CAII	1.00 ± 0.14	−3.86 ± 0.06	4.38	−8.24
4	CB[6]	3.61 ± 0.90	−2.08 ± 0.10	5.40	−7.48
	CAII	0.48 ± 0.07	−2.22 ± 0.02	6.45	−8.67
5	CB[6]	236 ± 30	−4.79 ± 0.66	0.20	−4.99
	Avidin [a]	≈ 10^{-19}	N.D.	N.D.	≈ −20

[a] Estimated values shown are based on measurements from Ref. [21].

Zn^{2+}-targeting moiety, as previously demonstrated for many CA inhibitors.[16] We therefore designed TFGs **1**–**4** (Table 1), which all have a CAII-binding *p*-benzenesulfonamide moiety and CB[6]-binding butylamine tail, but with varying length and chemical structure of the linker.

Synthetic details for TFGs **1**–**4** are provided in Scheme S2. Briefly, by following procedures modified from Salvatore et al.,[17] **1** and **2** were synthesized from the primary amine and alkyl bromide in a single step with cesium hydroxide monohydrate as the base in 30 % and 43 % yield, respectively. TFGs **3** and **4** were synthesized in two steps. In the first step, 2-chloroacetyl chloride was reacted with 4-(2-aminoethyl)benzenesulfonamide or 4-aminobezenesulfonamide in 68 % or 70 % yield and subsequently reacted with 1-butylamine to deliver **3** or **4** in 56 % or 50 % yield, respectively.

To test whether the TFGs function as desired in the prototypal CB[6] molecular relay, binding affinities were measured by ITC separately for CB[6] and CAII (Table 1 and Figure S1). The association constants for CB[6] titrated with **1**, **2**, **3**, or **4** were all in the range of 1–3 × 10^5 M^{-1} at 300 K in pH 7.2, PBS buffer with 1 % DMSO. We then performed ITC to test the binding of **1**–**4** to CAII in the same buffer, and **4** displayed the highest affinity. The likely origins of the enthalpic and entropic contributions towards the binding of **1** to CAII are observed in the crystal structure of the enzyme–TFG complex (Figure S2). The benzenesulfonamide moiety of **1** forms the interactions typically observed for arylsulfonamide inhibitors: the sulfonamidate nitrogen atom (N) coordinates to the catalytic Zn^{2+} and donates a hydrogen bond to the hydroxy oxygen of T199, and a sulfonamide oxygen atom accepts a hydrogen bond from the backbone amide nitrogen of T199. The *n*-butyl tail of **1** occupies a hydrophobic pocket lined by residues L198, P202, L204, F131, V135, and L141. Other sulfonamide inhibitors with flexible hydrophobic tails have also been observed to occupy this pocket.[18] The amine nitrogen in the tail of **1** is positioned near residues L198 and P202 but does not form hydrogen bonds with the protein or solvent. This limits enthalpic contributions to TFG binding, whereas solvent displacement contributes significant entropy to ΔG.

A crystal structure of CAII bound to the longest TFG (**3**; Figure 1) shows that the amine nitrogen is only 4.8, 5.1, and 5.4 Å from the three neighboring residues, respectively. Based

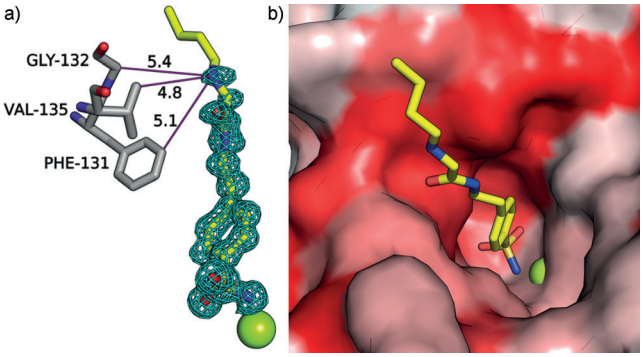

Figure 1. X-ray crystal structure of TFG **3** bound to CAII. a) A simulated annealing omit map (contoured at 3σ) shows **3** bound to Zn^{2+} (green sphere) in the active site of CAII. Interatomic distances (solid purple lines) are given in Å. Water molecules are omitted for clarity. b) The CAII active-site channel is represented as a surface model (hydrophobic residues in red; hydrophilic residues in white).

on these distances, TFG **3** is not available to bind simultaneously to CB[6], which has an outer diameter of 6.9 Å at its portal and 14.4 Å at its widest point.[19] Molecular modeling (Figure S3) helps to illustrate that a stable ternary structure cannot form between CAII, TFG **3**, and CB[6] owing to steric clashes. Finally, a crystal structure of CAII with TFG **4** (which lacks an ethyl linker), confirms that the butyl tail is even less solvent accessible in this complex (Figure S4).

The CB[6]–TFG complexes were incubated with CAII for 20 min, and the hydrolysis rates of *p*-nitrophenyl acetate (*p*NPA) enzymatically catalyzed by CAII were determined by monitoring an increase in absorbance at $\lambda = 400$ nm (Figure 2). Compounds **3** and **4** displayed stronger CAII inhibition compared to the other TFGs, which is consistent with their higher CAII affinity. CB[6] alone did not show any CAII inhibition, which suggests a lack of direct interaction between CAII and CB[6]. When complexed with CB[6], all of the TFGs inhibited CAII activity only slightly less than TFG alone, which provides further evidence that the TFGs shuttle from CB[6] to CAII, as designed. Furthermore, titration of CB[6] led to recovery of CAII activity (Figure S5), thus demonstrating that the shuttling of TFG is under thermodynamic control. This is also consistent with butylamine undergoing fast exchange ($\tau_{exch} < 10$ ms) with CB[6].[20]

Based on its highest affinity for CAII and intermediate affinity for CB[6] (Table 1), TFG **4** was selected for testing

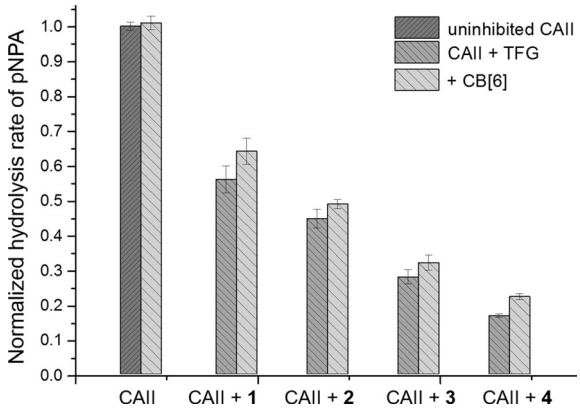

Figure 2. Comparison of CAII esterase activity with different TFGs and CB[6]–TFG complexes monitored by using *p*NPA as a substrate. All assays were performed after 20 min incubation. Standard errors were determined from three or more replicates for each condition.

our "turn-on" ^{129}Xe NMR biosensing strategy. First, 1 μM CB[6] was dissolved in pH 7.2 PBS solution, and multiple selective Dsnob-shaped saturation pulses were scanned over the chemical shift range of $\delta = 90$–230 ppm in 5 ppm steps. Two saturation responses were observed (Figure 3), centered

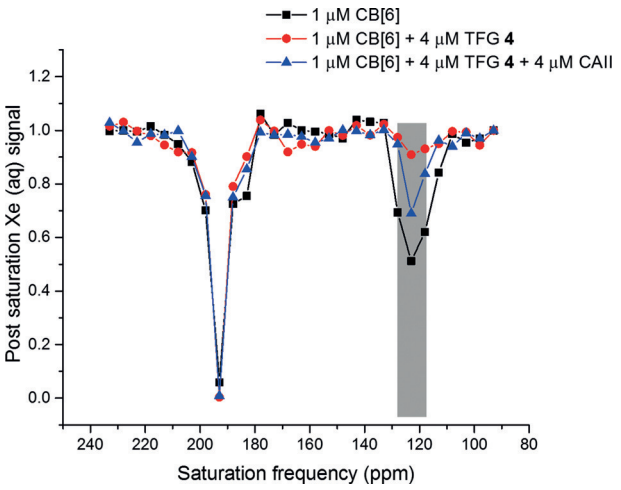

Figure 3. Frequency-dependent ^{129}Xe NMR saturation spectra in pH 7.2 PBS at 300 K show CAII detection through a CB[6]–**4** molecular relay.

at $\delta = 193$ ppm (^{129}Xe-aq) and 122 ppm (^{129}Xe-CB[6]). Upon addition of 4 μM TFG **4**, the ^{129}Xe–CB[6] Hyper-CEST signal at $\delta = 122$ ppm was greatly reduced as a result of less free CB[6] (ca. 0.5 μM) in the sample solution. Finally, when 4 μM CAII was added to the solution, the ^{129}Xe–CB[6] Hyper-CEST signal was mostly restored, thus confirming that TFG **4** was sequestered by CAII.

To apply the molecular relay to a system with different thermodynamic properties, we employed a commercially available pentylamine biotin (pAB) TFG **5** that binds CB[6] much less tightly than its target protein avidin. TFG **5** was determined by ITC (Table 1) to bind to CB[6] with modest affinity ($K_A = 4240\ M^{-1}$), whereas avidin affinity was estimated to be much higher ($K_A \approx 10^{14}\ M^{-1}$).[21] In order to block xenon access initially, we added 50 μM TFG **5** to 1 μM CB[6] solution, and as expected, the ^{129}Xe–CB[6] Hyper-CEST signal was completely turned off. Subsequently, administration of 50 μM avidin fully restored the ^{129}Xe–CB[6] signal (Figure 4). These data highlight the ease of reprogramming the CB[6]–TFG relay for assaying a wide range of biomolecules in solution.

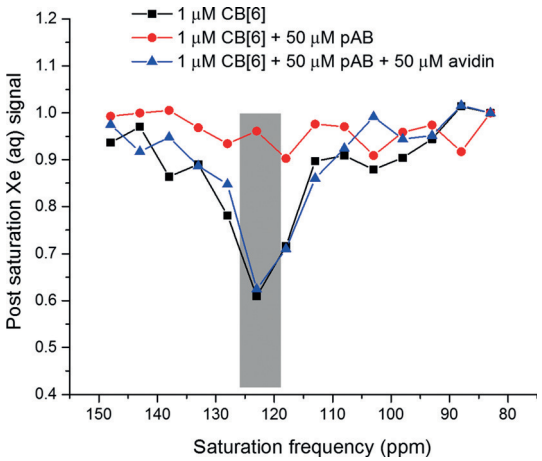

Figure 4. Frequency-dependent ^{129}Xe NMR saturation spectra in pH 7.2 PBS at 300 K show avidin detection through a CB[6]–pAB molecular relay.

Finally, we investigated our molecular relay in cellular environments. BL21(DE3) *E. coli* expressing recombinant CAII was cultured in LB medium and induced with 1 mM isopropyl β-D-1-thiogalactopyranoside (IPTG) and 1 mM $ZnCl_2$. Cells were then pelleted, washed, resuspended in PBS buffer, and lysed with two freeze–thaw cycles. Quantitative SDS gel analysis indicated expression levels of 12 nmol CAII (3 mL of 4 μM sample solution) from cell lysate equivalent to $OD_{600\,nm} = 2$ (Figure S6). Non-transformed *E. coli* were grown and lysed in the same manner to serve as a negative control. Screening experiments revealed that 16 μM CB[6] gave useful residual ^{129}Xe Hyper-CEST NMR signal, despite CB[6] binding to many components of the bacterial lysate. Addition of 4 μM TFG **4** to control sample with 16 μM CB[6] greatly reduced the Hyper-CEST signal, whereas in lysate from CAII-overexpressing *E. coli*, the original NMR signal intensity was observed (Figure 5). These experiments highlight the ability of the CB[6] detection approach to identify a specific protein target within a complex mixture. The molecular relay thus extends the utility of CB[6] for ultrasensitive ^{129}Xe NMR biosensing.

In summary, by exploiting versatile CB[6] host–guest chemistry and facile attachment of a CB[6]-binding domain to a protein-binding moiety, we were able to generate novel ^{129}Xe NMR biosensors. This work was guided by X-ray crystal structure determination of three CAII–TFG complexes.[22] The TFG programs the molecular relay for exquisite control over chemical equilibria between several interacting components: CB[6], TFG, the target molecule, and Xe. This strategy

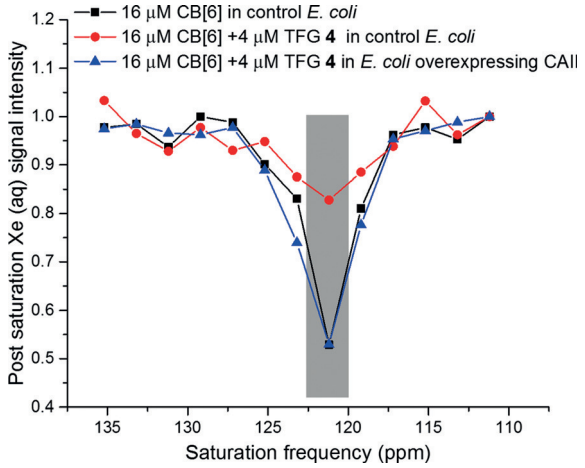

Figure 5. Frequency-dependent ^{129}Xe NMR saturation spectra show CAII detection through a CB[6]–**4** relay in bacterial lysate ($OD_{600\,nm} = 2$) at 300 K.

produces a CB[6]–^{129}Xe NMR signal and makes it possible to "target" CB[6] for specific biomolecule detection. In the Hyper-CEST setup, because Xe (ca. 136 μM, all isotopes) is more abundant than other components, analyte detection sensitivity should be maximized when the TFG is engineered to achieve well discriminated binding affinities: analyte–TFG ≫ CB[6]–TFG ≫ CB[6]–Xe. The thermodynamic and kinetic stability of the starting CB[6]–TFG complex will have additional significance for future in vivo applications in molecular imaging.

Acknowledgements

This work was supported by NIH R01-GM097478 and CDMRP-LCRP Concept Award no. LC130824. The ITC was purchased via NIH S10-DO016260. We thank Drs. George Furst and Jun Gu for assistance with NMR spectroscopy. We thank Dr. David Christianson for the CAII plasmid and assistance with crystallography. We thank the Stanford Synchrotron Radiation Lightsource (SSRL) and Advanced Photon Source (APS) for access to their respective beamlines for X-ray crystallographic data collection.

Keywords: bioinorganic chemistry · biosensors · host–guest systems · molecular recognition · NMR spectroscopy

How to cite: *Angew. Chem. Int. Ed.* **2016**, *55*, 1733–1736
Angew. Chem. **2016**, *128*, 1765–1768

[1] a) C. Y. Cheng, P. R. McGonigal, S. T. Schneebeli, H. Li, N. A. Vermeulen, C. F. Ke, J. F. Stoddart, *Nat. Nanotechnol.* **2015**, *10*, 547–553; b) G. M. Whitesides, B. Grzybowski, *Science* **2002**, *295*, 2418–2421; c) W. R. Browne, B. L. Feringa, *Nat. Nanotechnol.* **2006**, *1*, 25–35.

[2] a) Y. Wang, I. J. Dmochowski, *Chem. Commun.* **2015**, *51*, 8982–8985; b) M. Kunth, C. Witte, A. Hennig, L. Schröder, *Chem. Sci.* **2015**, *6*, 6069–6075.

[3] L. Schröder, T. J. Lowery, C. Hilty, D. E. Wemmer, A. Pines, *Science* **2006**, *314*, 446–449.

[4] a) J. Demarquay, J. Fraissard, *Chem. Phys. Lett.* **1987**, *136*, 314–318; b) P. Sozzani, S. Bracco, A. Comotti, M. Mauri, R. Simonutti, P. Valsesia, *Chem. Commun.* **2006**, 1921–1923.

[5] Y. Bai, Y. Wang, M. Goulian, A. Driks, I. J. Dmochowski, *Chem. Sci.* **2014**, *5*, 3197–3203.

[6] J. P. Mugler III, T. A. Altes, *J. Magn. Reson. Imaging* **2013**, *37*, 313–331.

[7] a) T. Brotin, J. P. Dutasta, *Chem. Rev.* **2009**, *109*, 88–130; b) O. Taratula, P. A. Hill, N. S. Khan, P. J. Carroll, I. J. Dmochowski, *Nat. Commun.* **2010**, *1*, 148.

[8] O. Taratula, P. A. Hill, Y. Bai, N. S. Khan, I. J. Dmochowski, *Org. Lett.* **2011**, *13*, 1414–1417.

[9] a) T. K. Stevens, R. M. Ramirez, A. Pines, *J. Am. Chem. Soc.* **2013**, *135*, 9576–9579; b) S. Klippel, C. Freund, L. Schröder, *Nano Lett.* **2014**, *14*, 5721–5726; c) M. G. Shapiro, R. M. Ramirez, L. J. Sperling, G. Sun, J. Sun, A. Pines, D. V. Schaffer, V. S. Bajaj, *Nat. Chem.* **2014**, *6*, 629–634.

[10] a) L. Isaacs, *Chem. Commun.* **2009**, 619–629; b) K. Kim, N. Selvapalam, Y. H. Ko, K. M. Park, D. Kim, J. Kim, *Chem. Soc. Rev.* **2007**, *36*, 267–279; c) S. Walker, R. Oun, F. J. McInnes, N. J. Wheate, *Isr. J. Chem.* **2011**, *51*, 616–624; d) A. Hennig, H. Bakirci, W. M. Nau, *Nat. Methods* **2007**, *4*, 629–632; e) J. M. Chinai, A. B. Taylor, L. M. Ryno, N. D. Hargreaves, C. A. Morris, P. J. Hart, A. R. Urbach, *J. Am. Chem. Soc.* **2011**, *133*, 8810–8813.

[11] a) A. C. Bhasikuttan, J. Mohanty, W. M. Nau, H. Pal, *Angew. Chem. Int. Ed.* **2007**, *46*, 4120–4122; *Angew. Chem.* **2007**, *119*, 4198–4200; b) D. V. Berdnikova, T. M. Aliyeu, T. Paululat, Y. V. Fedorov, O. A. Fedorova, H. Ihmels, *Chem. Commun.* **2015**, *51*, 4906–4909; c) S. Ghosh, L. Isaacs, *J. Am. Chem. Soc.* **2010**, *132*, 4445–4454.

[12] B. S. Kim, Y. H. Ko, Y. Kim, H. J. Lee, N. Selvapalam, H. C. Lee, K. Kim, *Chem. Commun.* **2008**, 2756–2758.

[13] W. L. Mock, N. Y. Shih, *J. Org. Chem.* **1986**, *51*, 4440–4446.

[14] J. M. Chambers, P. A. Hill, J. A. Aaron, Z. H. Han, D. W. Christianson, N. N. Kuzma, I. J. Dmochowski, *J. Am. Chem. Soc.* **2009**, *131*, 563–569.

[15] C. T. Supuran, *Nat. Rev. Drug Discovery* **2008**, *7*, 168–181.

[16] J. M. Gao, S. Qiao, G. M. Whitesides, *J. Med. Chem.* **1995**, *38*, 2292–2301.

[17] R. N. Salvatore, A. S. Nagle, K. W. Jung, *J. Org. Chem.* **2002**, *67*, 674–683.

[18] a) D. Elbaum, S. K. Nair, M. W. Patchan, R. B. Thompson, D. W. Christianson, *J. Am. Chem. Soc.* **1996**, *118*, 8381–8387; b) M. Bozdag, M. Pinard, F. Carta, E. Masini, A. Scozzafava, R. McKenna, C. T. Supuran, *J. Med. Chem.* **2014**, *57*, 9673–9686.

[19] a) D. Bardelang, K. A. Udachin, D. M. Leek, J. A. Ripmeester, *CrystEngComm* **2007**, *9*, 973–975; b) J. W. Lee, S. Samal, N. Selvapalam, H. J. Kim, K. Kim, *Acc. Chem. Res.* **2003**, *36*, 621–630.

[20] W. L. Mock, N. Y. Shih, *J. Am. Chem. Soc.* **1989**, *111*, 2697–2699.

[21] N. M. Green, *Biochem. J.* **1963**, *89*, 585–591.

[22] The atomic coordinates of three complexes of human carbonic anhydrase II with sulfonamide TFGs have been deposited in the Protein Data Bank with accession codes 5EKH, 5EKJ, and 5EKM.

Received: September 25, 2015
Published online: December 21, 2015

